INVESTIGATION ON VIBRATION BEHAVIOUR AND DRIVING FORCES FOR FUEL ELEMENT MODELS IN PARALLEL FLOW

E. OHLMER, R. SCHWEMMLE

Commission of the European Communities,
Technology Division, EURATOM Joint Research Center, I-21020 Ispra (Varese), Italy

SUMMARY

Experiments on a fuel element model in the form of a simple three-rod bundle have been performed in water flow. The pressure difference fluctuations on the rod surface acting as the driving forces as well as the resulting lateral vibrations were measured by means of one instrumented rod. The pitch width of the bundle arrangement was varied and also the measurement direction of the instrumented rod. With this, the rod vibrations and pressure fluctuations could be determined in different directions with respect to the flow subchannels.

Previous measurements by the same instrumented rod in a single rod test facility proved the applicability of analytical models to predict the parallel flow induced rod vibrations. Such analytical models which describe by means of the Power-Spectral-Density functions the rod vibration as the response to the random pressure fluctuations, however, need complex quantities as input data. It is difficult, if not impossible today to obtain these quantities for arbitrary flow geometries in an analytical way. They are mainly the driving forces expressed by the intensity and frequency distribution of the pressure fluctuations in the boundary layer as well as the correlation coefficient of the pressure fluctuation field. But also the response function of the rod vibration could be influenced by the bundle arrangement, due to coupling and damping effects.

In this connection, the rod bundle experiment brought on the following points:

— The pressure fluctuations in the rod bundle are different from those in the single rod test. In the asymmetric flow geometry additional pressure fluctuations with a marked velocity depending frequency were found. Furthermore, the driving forces do not remain equal over the rod circumference.
— The correlation coefficient turns out to be influenced by geometric and hydrodynamic parameters.
— The response function of the rod vibration in the bundle is not equal in all directions of the cross section, and changes with the pitch width.

In order to investigate the driving forces of the rod vibration in more detail, coherence and phase shift of the pressure fluctuations have been measured in the length direction.

Finally, an attempt has been made to develop relations describing the influence of geometric parameters such as excentricity and local hydraulic diameters of the flow cross sections with respect to the driving forces.

1. Introduction

For the analytical determination of parallel flow induced vibrations of the rods in reactor fuel elements, mathematical models have been developed and experimentally checked by several investigations (see e.g. Chen, Wambsganss [1], or studies performed at the JRC [2], [3]). The derived formulas however, describing the involved phenomena from a theoretical point of view in a satisfying manner, do not resolve completely the problems in predicting the flow induced rod vibrations: As input data, these models need some complex quantities, which to-day for many practical cases may be difficult to obtain in an analytical way.

In order to achieve a better understanding of what kind these quantities are, one of the analytical models in the form as derived in [3] is briefly analyzed here. The general relation however, is rather complex and simplifying assumptions must be introduced for practical purposes in order to get a handling formula like:

$$\Phi_{y(\xi,\omega)} = K^2_{(\xi)} \left(\frac{\Delta \ell}{\ell}\right)^2 H^2_{(\omega)} F_{(a,p)} \qquad (1)$$

Herein the rod displacement y in the form of the Power Spectral Density (PSD) function $\Phi_{y(\omega)}$ is related by means of the mechanical rod response function $H_{(\omega)}$ to the driving forces expressed by $F_{(a,p)}$. The constant K contains apart from mechanical rod parameters, also the proportionality coefficient $\varkappa$, relating the driving forces to the exciting pressure fluctuations at the rod surface. See annexed list for the meaning of the other utilized symbols.

The expression $F_{(a,p)}$ results from a partial integration process of the double integral over the pressure fluctuation field on the rod surface in the length direction. Hereby, for each of the assumed N equal rod length sections $\Delta \ell_i$, the pressure fluctuation field p_i is supposed to be homogeneous and the modal values of the vibration a_i to be constant. Thus:

$$F_{(a,p)} = (a_1, a_2, \ldots a_N) \cdot \begin{vmatrix} \Phi_{11} & \Phi_{12} & \cdots & \Phi_{1N} \\ \Phi_{21} & \Phi_{22} & \cdots & \Phi_{2N} \\ \cdots & \cdots & \cdots & \cdots \\ \Phi_{N1} & \Phi_{N2} & \cdots & \Phi_{NN} \end{vmatrix} \cdot \begin{Bmatrix} a_1 \\ a_2 \\ \cdot \\ a_N \end{Bmatrix} \qquad (2)$$

with Φ_{ij} the PSD-functions (for i=j) respectively the Cross Spectral Densities (for i≠j) of the pressure fluctuations(±) measured in N points over the rod length.

Assuming furthermore an invariable pressure fluctuation field with respect to the rod length, the expression (1) can be reduced, considering N = 1 and $\Delta \ell = \ell$ respectively, to the even simpler form:

$$\Phi_{y(\xi,\omega)} = K^2_{(\xi)} H^2_{(\omega)} \Phi_{p(\omega)} \qquad (3)$$

(±) Note: "Pressure Fluctuations" means throughout this paper the fluctuations of the pressure difference between two opposite points of the rod cross section, as they act as driving forces.

In this case the driving forces are represented by the PSD-function $\Phi_{p(\omega)}$ of the pressure difference fluctuations determined in only one arbitrary section of the rod length.

For practical applications the driving forces, expressed by the intensity and by the frequency distribution of the random pressure difference fluctuations (like $F_{(a,p)}$ or $\Phi_{p(\omega)}$) must be known. Actually, no method is available for their analytical evaluation in an arbitrary flow geometry. An analogous statement can be made as far as the coefficient χ is concerned. On the other hand, the response function $H_{(\omega)}$ of the single rods inside the complex structure of a fuel element bundle is possibly not well defined.

2. Experimental Facility

For a more detailed description of the experimental facility reference is made to [4]. Here, only a few points of importance are presented.

2.1 Test Section. The bundle model is formed by three equal rods (brass tube Ø 18x15 mm, 1 m long), one of which is the instrumented test rod whereas the others are both dummy rods (Fig. 1). The bundle is mounted in a flow channel (50 mm inside diam.) by means of two grids, giving a hinged end fixation for the rods. The hydraulic diameter results to be 14.7 mm.

The distance between the rods in the bundle arrangement can be varied by means of slotted guides in the grids. Furthermore, the instrumented rod could be rotated with a special device (Fig. 4). Thus, the pressure transducers, mounted all in the same plane along the rod, could be aligned to different directions in the flow subchannels.

The turbulence driving forces are measured as the momentary difference of the pressure fluctuations on the rod surface between diametrically opposite points in the cross section. Correspondingly, 5 pairs of miniature pressure transducers (Type CQL-080, Kulite, with 1.8 mm membrane diameter) were mounted in equidistant positions over the rod length (Fig. 2). The rod vibration is measured by a couple of strain-gauges applied to the center of the length at the inner rod wall, in the same plane as the pressure transducers.

For the coherence measurements of the pressure field, the actual test rod was exchanged for another rod with the same dimensions but with a different instrumentation: one pair of pressure transducers was fixed at the position $\xi = 0.7$ as reference point. Two other pairs could be mounted at different distances, varying from 7 up to 68 mm downstream from the reference point (Fig. 3). No vibration measurement could be made in this case.

2.2 Signal Processing. The signal analysis concerns mainly the intensity (RMS-values) and the frequency distribution (PSD-diagrams) of the tape-recorded signals. The function $F_{(a,p)}$, as derived for the mathematical model in eq. (2), is the PSD-function of the sum of all the pressure difference signals measured over the rod length and weighted by the corresponding modal values a_i. This weighting and summation operation can be performed easily with the method described in [3].

2.3 Test Loop. The test channel is connected by piping directly to the main water line coming from a storage tank. In this way no pumps were needed for the water circulation. The flow velocity in the test section has been varied in the range between 5.5 and 11.7 m/sec, corresponding to Re numbers of about $5.7 \cdot 10^4$ to $1.2 \cdot 10^5$.

3. Results

In the following, mainly the influence of the geometric and hydrodynamic parameters on the rod vibration and on the pressure fluctuations is analyzed. Fig. 5 shows the flow geometries for the 4 investigated pitch widths γ and also the definition of the angular direction of the measurement plane.

3.1 Rod Vibration. The intensity of the rod vibration strain ε is represented as the RMS-values normalized by a reference strain ε^*. The reference value, calculated as the flexural strain due to the hypothetical static load $F_{n(\xi)} = a_{n(\xi)} \cdot q \cdot D$, is proportional to the dynamic pressure q and to the considered vibration mode a_n.

The normalized rod vibration intensity nearly remains constant in the investigated Re-range, as shows Fig. 6. Hence, the intensity increases proportional to v^2. But one appreciates an important influence of the pitch width γ. Typically, the lowest intensity is found for $\gamma = 1.25$, that means for the bundle arrangement, where the rods are relatively well centered with respect to the surrounding flow subchannels.

Compared with the values of the previous single rod experiment, the vibration intensity is increased in the bundle test. Two causes may be responsible for this: firstly, the response function of the rods in the bundle is enlarged by coupling effects. Thus, vibration energy from the pressure fluctuations is accepted in a larger frequency band. Secondly, the proportionality coefficient $\varkappa$ was found to be higher for the bundle arrangement than for the single rod test.

Furthermore, the vibration intensity is not equal in all directions, see Fig. 7. The direction to the bundle center ($\varphi = 90^\circ$) is a plan of symmetry and gives the lowest vibrations. Compared to this, the vibration intensity increases up to about 30% when measured in the direction to the external subchannels.

The inspection of the frequency distribution (Fig. 8) shows that the rod vibrates at different frequencies depending on the geometric parameters: the frequency of about 33 Hz is present more or less in all conditions, but mainly in the direction to the bundle center. Changing the direction towards the external subchannels, and for higher rod distances, this frequency decreases for the benefit of other, slower frequencies. This behaviour will be discussed in connection with the response function measurements in chapter 4.

3.2 Difference Pressure Fluctuations. The lowest RMS-values of the pressure fluctuations were found for the direction to the bundle center and for the pitch width giving the most regular flow cross sections ($\gamma = 1.25$), see Fig. 9. In this case the RMS-values, normalized

by the dynamic pressure q agree well with the commonly accepted magnitude of turbulent pressure fluctuations. (Note that the RMS-values resulting as the difference between two pressure fluctuations are greater by a factor $\sqrt{2}$ than the values from one side only). The slow decrease of the normalized intensity for increasing Re numbers, indicating a dependency proportional to the flow velocity with exponent of about 1.5 to 1.8, is also in agreement with the results of other studies.

The turbulence intensity however, seems increased significantly (as shows Fig. 9), when the bundle arrangement produces a more excentric flow geometry. Furthermore, one notices a considerable difference in the pressure fluctuations over the cross section, see Fig. 10. The increase by a factor of about 1.6 is higher than found before for the rod vibration. Fig. 11 shows the importance of measuring the pressure by difference signals. The signals of the single transducers are affected mainly in the lower frequency range, by static pressure fluctuations of the loop and by far-field noise, which do not act as driving forces and which are cancelled by the difference process. Thus, the single signals can not be representative for the excitation of the rod vibration.

The most striking property observed in the PSD diagrams is the appearance of a fluctuation peak in a certain frequency range. (Fig. 12). Such a peak has never been observed in the previous single rod test, where the pressure fluctuations yielded a regular PSD-curve of a slowly decreasing white noise. Now, in the bundle arrangement a pressure pulsation in a defined frequency range seems to overlay the white noise turbulence structure. This behaviour comes out quite clearer in the direction of the external subchannels and in this way increases the intensity values as stated before.

Comparing the PSD-plots for different pitch widths, Fig. 13, the turbulence pulsations seem to be influenced significantly by the changes of the flow geometry.

The frequency of the dominant pulsations varies linearly with the flow velocity, see Fig. 14. This may be of importance, whenever the eigenfrequencies of the affected structures lie in the shift range during flow variations. In this case, the observed proportionality between vibration amplitude and v^2 will certainly be modified.

For the analytical model, see chapter 1, the function $F_{(a,p)}$ was derived, which corresponds to the weighted sum over all measured pressure difference signals. As an example, a plot of this function is given in Fig. 15. This curve is similar to the PSD-plots of the local pressure differences, except several peaks and valleys at certain frequencies. These frequencies are in a clear relation to the flow velocity and to the transducer distances. This effect gives a first indication for a strong length correlation of the pressure fluctuation field, which will be proved more precisely by the coherence measurements in the following.

4. Determination of the Response Function

This test was performed with the test section under the same conditions as the flow test

but in stagnant water (Fig. 16). It was not possible to obtain a clear result with an incontestable and reproducible resonance frequency, see e. g. Fig. 17a. Obviously, the test rod is strongly influenced by the two other rods in the bundle. Only when the two dummy rods have been blocked to covibrate, definite resonance curves could be obtained. These curves (see Fig. 17b) show that the rod vibration in the bundle is strongly damped and that the damping changes with the pitch width.

More realistic response functions have been evaluated from the flow tests. In fact, as the PSD-functions of the rod vibration and of the pressure fluctuations are supplied by these tests, the response function can be calculated applying the analytical model for instance of eq. (1). These calculated values $h_{(\omega)}$ show, (Fig. 18), that the response function for the rod in the bundle has not a unique form for all directions and beyond this, changes with the pitch width. One can distinguish mainly two different resonance frequencies:

- the lower one, present mainly in the tangential direction ($\varphi = 30^{\circ}$ or 150°) can be identified as the initial rod eigenfrequency. This frequency varies with the pitch width between about 24 and 28 Hz, which agrees with the result of the resonance tests;
- the vibration at ~ 33 Hz can be interpreted as a vibration mode of the bundle as an ensemble. In fact, this vibration is present mainly in the direction of the bundle center and increases with decreasing rod distance.

5. Proportionality Coefficient

The coefficient $\varkappa$ can be evaluated in an analogous manner with the analytical model introducing the experimental data as above. This evaluation however, is based upon the assumption, that $\varkappa$ is not a function of frequency, as still supposed in the model. The following values have been determined:

Influence of flow velocity v		Influence of direction φ		Influence of pitch width γ		
V (m/sec)	$\varkappa$	φ ($^{\circ}$)	$\varkappa$	γ	$\varkappa$ ($\varphi = 90^{\circ}$)	$\varkappa$ ($\varphi = 30^{\circ}$)
single rod						
9.0	0.03					
7.5	0.03	30	0.125	1.05	0.11	0.095
5	0.02	60	0.16	1.15	0.095	0.08
rod bundle		90	0.165	1.25	0.165	0.12
11.2	0.18					
10.0	0.16	120	0.13	1.35	0.17	0.15
6.6	0.13	150	0.12			

One can state the following:

- The coefficient $\varkappa$ is found to be higher in the rod bundle than in the single rod test. This may be due to the additional pulsations with the strong length correlation as discussed be-

fore.

- $\varkappa$ Increases with the flow proportional to the velocity with the exponent of about 0.8.

- The variation with the direction φ may be explained by the geometric distribution of the unequal driving forces over the rod cross section. This distribution dependency which should not be confounded with a correlation effect of the pressure field, can be expressed by:

$$\frac{\varkappa_{(\varphi_i)}}{\bar{\varkappa}} = \frac{1}{2}\int_0^{\pi} \frac{\overline{\Delta_p}}{\Delta_{p_{(\varphi)}}} \sin\varphi \, d\varphi \qquad ; \text{ with } \varphi = \varphi_i - \pi/2$$

Here, $\Delta_{p_{(\varphi)}}$ stands for the local driving forces ($\triangleq$ the RMS pressure difference fluctuations) and $\bar{\varkappa}$ and $\overline{\Delta_p}$ are mean values over the rod circumference.

6. Coherence Measurements of the Pressure Field

The proportionality factor $\varkappa$ in the analytical model plays the role of a correlation coefficient for the pressure fluctuation field. In fact, as evaluated above, this coefficient gives the proportionality between the pressure fluctuations revealed experimentally in one or even in several points over the rod length and the resulting total driving forces. In this way, it takes account of the existing correlation of the pressure field over the rod surface. Inversely, when evaluating the driving forces mathematically on the basis of a known PSD function of the pressure fluctuations in one point, one needs knowledge about the correlation between this single statistical data and the surrounding pressure field, as well as the magnitude and as the phase shift concerned.

The magnitude of the correlation can be defined by the coherence. As is well known, the coherence is a frequency function with values between 0 and 1 as given by

$$\gamma^2_{(\omega)} = \frac{\left|\Phi_{ij_{(\omega)}}\right|^2}{\Phi_{ii_{(\omega)}} \Phi_{jj_{(\omega)}}}$$

Properly this information about the frequency distribution for the relation between the two considered pressure measurement points seems of advantage in front of the correlation measurements in the time domain still utilized in this frame by several researchers.

The measurements of coherence and of phase shift of the pressure difference fluctuations were made with a fixed pitch of 1.31 and only in the two directions $\varphi = 90^{\circ}$ and 150°. Fig. 19 shows some typical plots of the obtained data.

Significant coherence values are observed only up to about 500 Hz for the shorter distances. But also for the largest distance investigated, 68 mm, the coherence remains relatively high in the lower frequency range, typically in the zone of the dominant pressure pulsations when measured in the direction to the external subchannels.

As one may expect, the phase lag ψ is in a clear relation to the transducer distance δ, to the frequency and to the flow velocity as given by:

$$\psi = \frac{\delta \cdot \omega}{\beta \cdot v}$$

The factor β takes into account that the transport velocity for the turbulence eddies is lower than the mean flow velocity v. This factor was found in the order of 0.9 to 1.0.

In order to reassume the measured coherence values in a representative form, the mean values $\overline{\gamma}$ have been determined from the γ^2-diagrams by smoothing the plotted curves. The mean values were evaluated for the frequency range from 20 Hz up to the limit, where they fall under the significance level of about $\gamma^2 \lesssim 0.1$. The results are shown in Fig. 20.

One can assume an exponential relation between the mean coherence and the relative distance $\delta^{\pm} = \delta / d_h$ of the form:

$$\overline{\gamma} = e^{-c\,\delta^{\pm}}$$

The decay constant c results for this relation in the order of 0.16 to 0.28. The relatively high coherence level seems surprising. Therefore, some doubts have risen, whether the far-field noise was cancelled correctly by the difference setting of the signals for each transducer pair. But in this case, considering the different propagation mechanism for the far-field noise, the phase behaviour should be different from the measured one.

The frequency range for the significant coherence values seems relatively well defined by the dimensionless presentation over the Strouhal number $S = f \cdot d_h / v$, as shows Fig. 21.

7. Discussion

As stated at the beginning, applying mathematical models to predict the parallel flow induced vibrations in rod bundles, one may meet with three of the needed input data which are not easy to assess in an analytical way: The response function of the rods, the expression for the pressure fluctuations and the correlation coefficient.

The experiment pointed out that all these three magnitudes are more or less strongly influenced by the parameters of the bundle geometry. As a consequence it was found that the resulting rod vibration intensity under constant flow velocity increased by a factor of about 3 only by changing the bundle parameters in the investigated range. This increase is mainly due to an analog increase of the pressure fluctuations, but also the variations of the response function and of the correlation coefficient do contribute.

So far as the pressure fluctuations are concerned, their intensity seems to vary as well with the mean excentricity E of the flow cross section (whenever the pitch width varied) as with the local hydraulic diameter $d_h^{\pm}$ (whenever the direction φ was changed). This behaviour can be described by an empirical relation of the form:

$$\frac{\Delta p_{RMS}}{q} \hat{=} F\left(1 + E \frac{\overline{d_h^{\pm}}}{d_h}\right) ,$$

as shows Fig. 22; with: - $E = \frac{1}{\varphi} \int \frac{\Delta d_h^{\pm}}{d_h} \, d\varphi$, the mean excentricity of the flow cross section,

- $d_h^{\pm}$ = the local hydraulic diameter,
- $\overline{d_h^{\pm}}$ = the mean value of $d_h^{\pm}$ for a subchannel,
- $\Delta d_h^{\pm} = \left| d_{h(\varphi)}^{\pm} - d_{h(\varphi+\pi)}^{\pm} \right|$

Evidently, such a purely empirical relation is not satisfying as a general solution. Thus an attempt was made to describe the pressure fluctuation intensity by the local wall shear stresses in the boundary layer, which gives satisfying preliminar results. This study however, is not yet completed. Eventually, it should be possible as well to relate the observed frequency behaviour of the fluctuations to the vortex generation in the boundary layer.

For the coefficient χ, the dependency of the flow velocity as well as of the unequal pressure distribution has been pointed out. An empirical relation to the excentricity and to the local hydraulic diameters could be derived as before for the fluctuation intensity. But a better approach for this point will probably be furnished by further investigations of the coherence of the pressure field. The actual results show a clear relation for the phase shift and a certain tendency for the length decay and for the frequency behaviour of the coherence values. But the actual coherence results, even if significant, are rather scattered. This is probably due to the fact, that following the underlying concept of the difference values for the pressure fluctuations, in each coherence evaluation the signals enter from four single pressure transducers. Thus for the accuracy one has to consider all the connected problems of calibration and mutual adjustment of the instrumentation as well as the statistical precision. Especially further coherence studies have to investigate in more detail the influence of geometric parameters for complex flow geometries.

The evaluation of the rod response function finally is a mechanical problem. Several codes exist for the calculation of the eigenfrequencies and vibration modes of mechanical structures. But one has to consider that following the presented results, the response function of the rod in a bundle is quite different from that of an isolated rod. Thus, the corresponding coupling and damping effects have to be introduced in the codes for reliable applications.

Acknowledgement

The experiments of the coherence measurements have been designed and performed in straight collaboration with Dr. J. Kadlec and Mr. K. D. Appelt from the JRE, Kernforschungszentrum, Karlsruhe. The coherence measurements on the signals were made by Mr. De Concini and Mr. P. Gori of the CNEN in Bologna. The authors acknowledge their precious support.

List of Symbols

a_n	normal vibration modes	v	flow velocity
d_h	hydraulic diameter	y	rod flexural displacement
D	rod diameter	$\varepsilon, \varepsilon^{\pm}$	strain, reference strain
f	frequency	$\varkappa$	proportionality factor for driving forces
h, H	frequency response function	ω	circular frequency
K =	$\frac{a}{M}(\xi)\frac{D\ell}{\omega_1^2}\cdot\varkappa$	$\xi = \frac{y}{\ell}$	adimensional length variable
$\ell, \Delta\ell$	rod length, partial length	φ	measurement direction
M	generalized mass	γ	pitch width
N, n	number	$\gamma^2_{(\omega)}, \bar{\gamma}$	coherence function, mean coherence
p, Δp	pressure difference fluctuations		
q	dynamic pressure		

References

[1] CHEN, WAMBSGANSS; "Parallel-flow-induced Vibrations of Fuel Rods". Nucl. Eng. & Design, 18 (72) 253 ff

[2] S. RUSSO; "Studio teorico-sperimentale delle vibrazioni indotte dalle flutuazioni di pressione in elementi cilindrici di combustibile nucleare immersi in un refrigerante liquido assiale." EUR-4815 (1972)

[3] OHLMER, RUSSO, SCHWEMMLE; "Investigation of an Analytical Model for Parallel-flow-induced Rod Vibrations." Nucl. Eng. & Design, 22 (1972) No. 2

[4] OHLMER, SCHWEMMLE; "Untersuchung der hydrodynamischen Schwingungsanregung an einem Dreier-Stabbündel unter achsparalleler Wasserströmung." EUR-4945 d (1973)

Fig. 1 : Three rod bundle

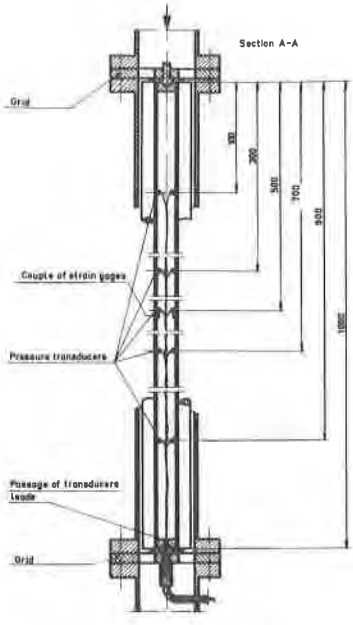

Fig. 2 : Rod instrumentation

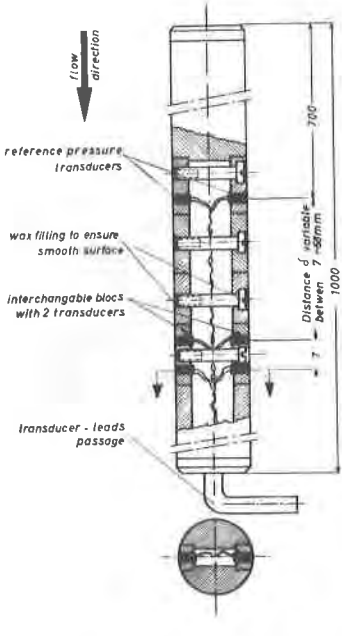

Fig. 3 : Instrumentation for coherence measurements

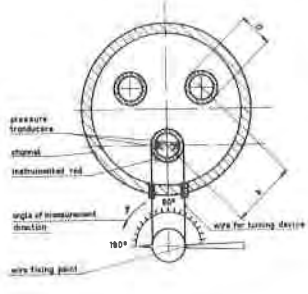

Fig. 4 : Rod turning device

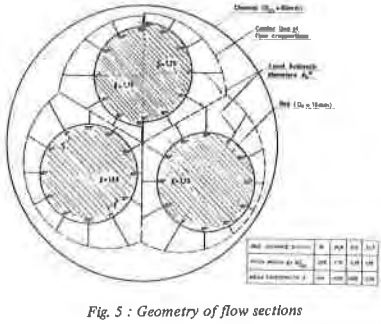

Fig. 5 : Geometry of flow sections

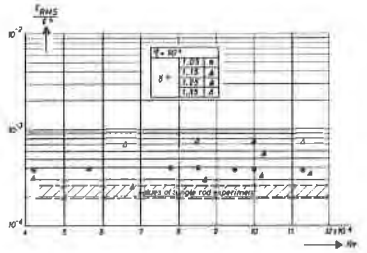

Fig. 6 : Normalized RMS-values of the rod vibration strain

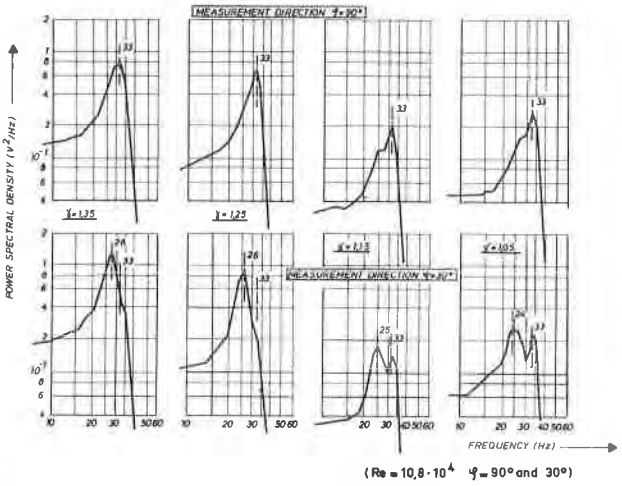

Fig. 8 : PSD-plots of rod vibration strain

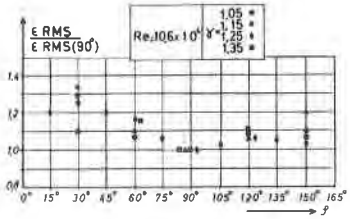

Fig. 7 : Vibration intensity varying with direction

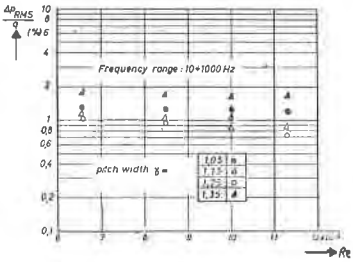

Fig. 9 : Normalized RMS-values of the pressure difference fluctuations

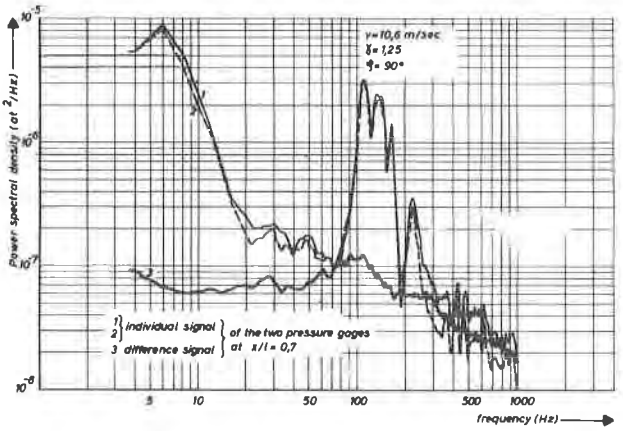

Fig. 11 : PSD-plots pressure fluctuations (single and difference signals)

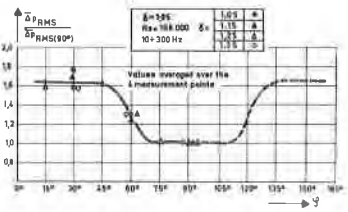

Fig. 10 : Intensity of pressure fluctuations varying with direction

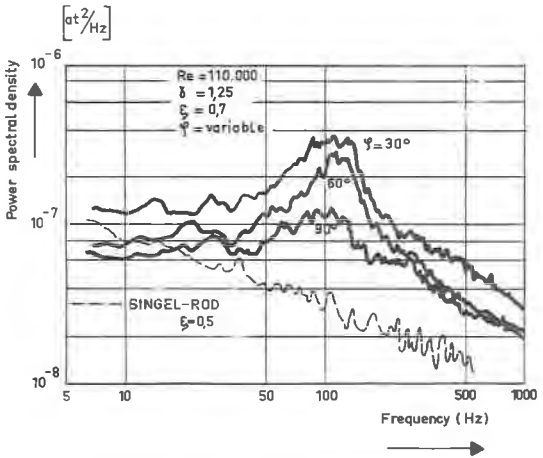

Fig. 12 : PSD of pressure diff. fluctuations for different directions

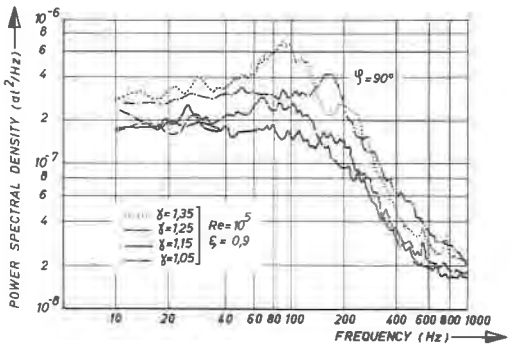

Fig. 13 : PSD of pressure diff. fluctuations for different pitch widths

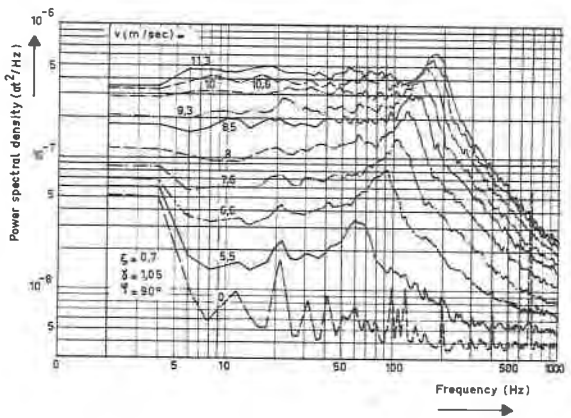

Fig. 14 : Influence of flow velocity on the pressure difference fluctuations

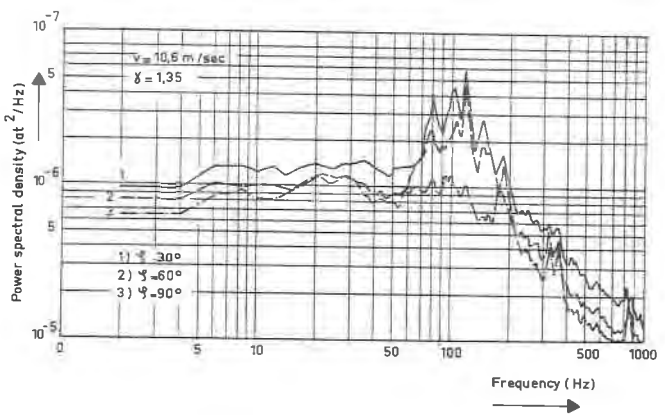

Fig. 15 : Plot of the driving force expression F(a, p)

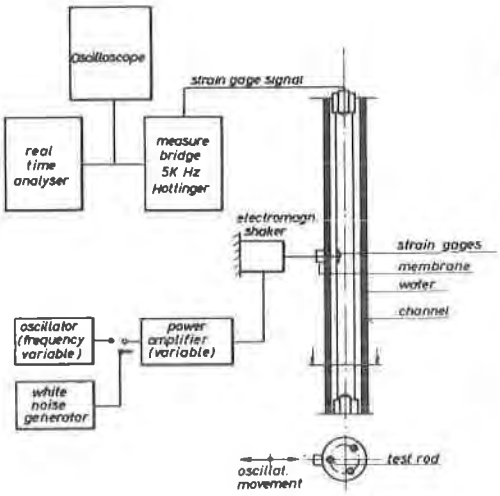

Fig. 16 : Frequency response measurements

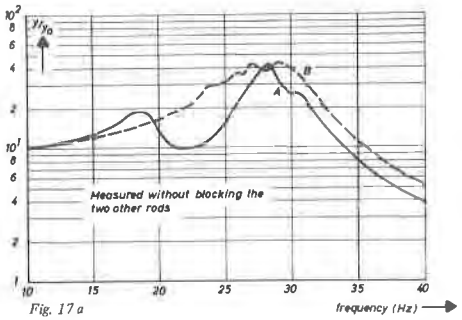

Fig. 17 a

Response functions measured in stagnant water

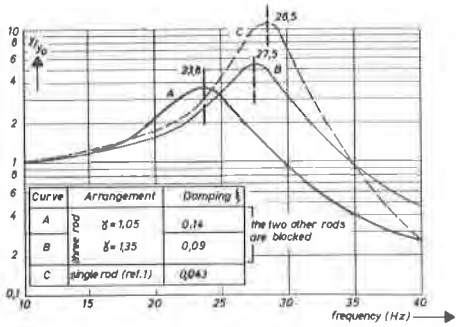

Fig. 17 b

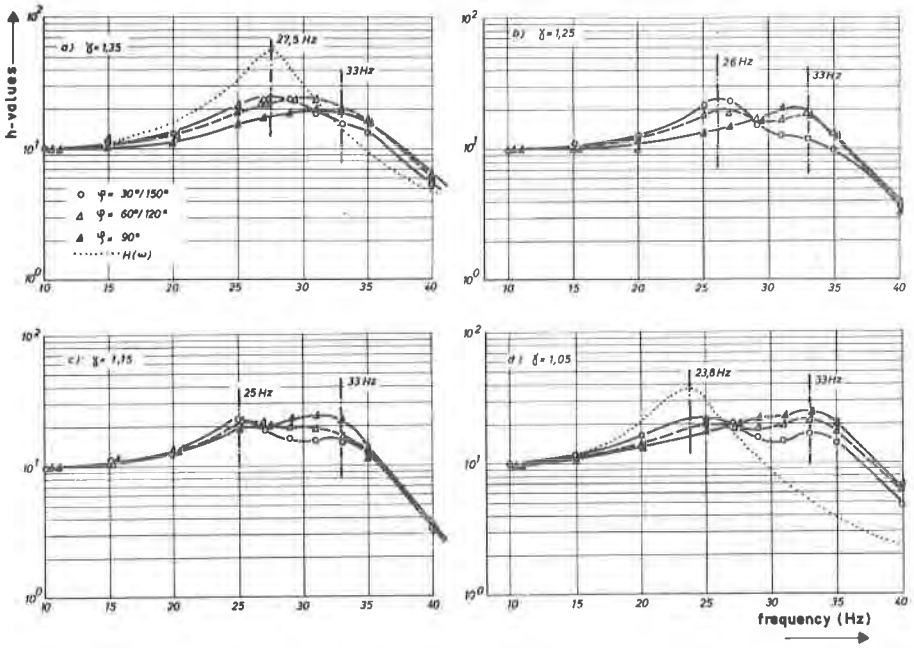

Fig. 18 : Response functions evaluated from flow test results

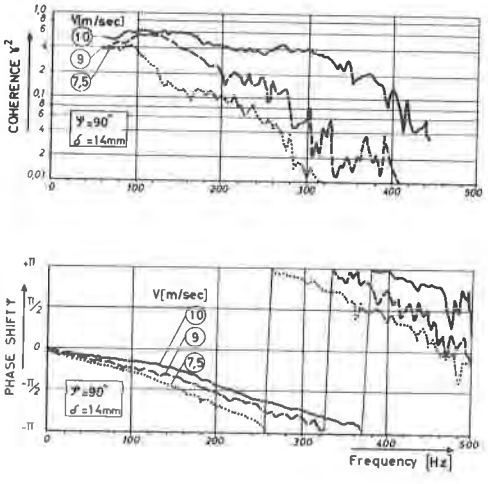

Fig. 19a : Typical coherence and phase diagrams

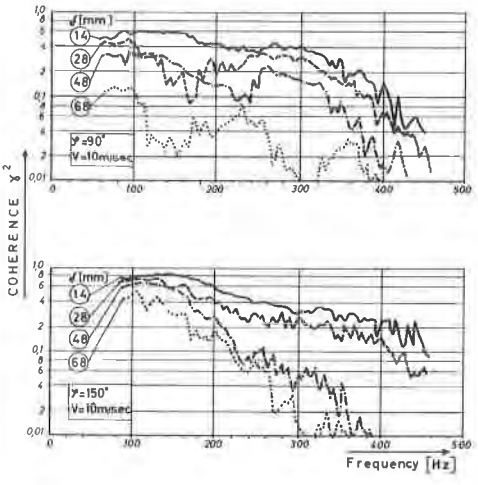

Fig. 19b : Typical coherence and phase diagrams

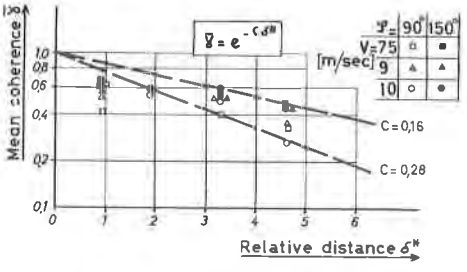

Fig. 20 : Mean coherence values as function of distance

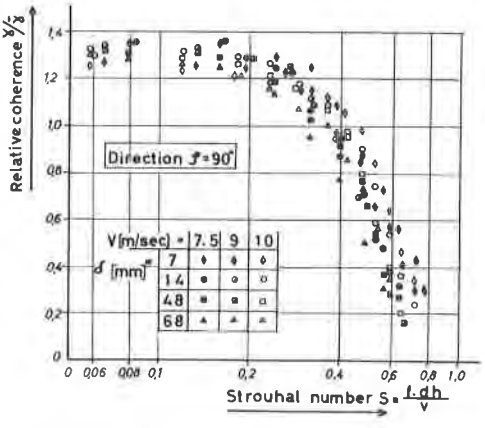

Fig. 21 : Relative coherence values as function of the Strouhal-number

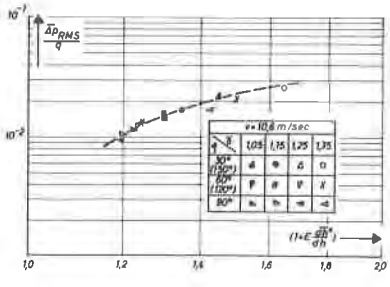

Fig. 22 : Intensity of pressure fluctuations as function of flow geometry parameters